HHS Public Access

Author manuscript

Gene Ther. Author manuscript; available in PMC 2023 August 01.

Published in final edited form as:

Gene Ther. 2023 August ; 30(7-8): 543–551. doi:10.1038/s41434-022-00321-w.

Targeting mAKAPβ Expression as a Therapeutic Approach for Ischemic Cardiomyopathy

Eliana C. Martinez[1], **Jinliang Li**[1,2], **Jennifer Arthur Ataam**[3], **Kristin Tokarski**[4], **Hrishikesh Thakur**[1,2], **Ioannis Karakikes**[3], **Kimberly Dodge-Kafka**[4], **Michael S. Kapiloff**[1,2,*]

[1]Interdisciplinary Stem Cell Institute, Department of Pediatrics, Leonard M. Miller School of Medicine, University of Miami, Miami, FL 33101

[2]Departments of Ophthalmology and Medicine, Stanford Cardiovascular Institute, Stanford University, Palo Alto, CA 94304

[3]Department of Cardiothoracic Surgery and Stanford Cardiovascular Institute, Stanford University, Stanford, CA 94305

[4]Calhoun Center for Cardiology, University of Connecticut Health Center, Farmington, CT 06030

Abstract

Ischemic cardiomyopathy is a leading cause of death and an unmet clinical need. Adeno-associated virus (AAV) gene-based therapies hold great promise for treating and preventing heart failure. Previously we showed that muscle A-kinase Anchoring Protein β (mAKAPβ, AKAP6β), a scaffold protein that organizes perinuclear signalosomes in the cardiomyocyte, is a critical regulator of pathological cardiac hypertrophy. Here, we show that inhibition of mAKAPβ expression in stressed adult cardiomyocytes *in vitro* was cardioprotective, while conditional cardiomyocyte-specific *mAKAP* gene deletion in mice prevented pathological cardiac remodeling due to myocardial infarction. We developed a new self-complementary serotype 9 AAV gene therapy vector expressing a short hairpin RNA for mAKAPβ under the control of a cardiomyocyte-specific promoter (AAV9sc.shmAKAP). This vector efficiently downregulated mAKAPβ expression in the mouse heart *in vivo.* Expression of the shRNA also inhibited mAKAPβ expression in human induced cardiomyocytes *in vitro.* Following myocardial infarction, systemic administration of AAV9sc.shmAKAP prevented the development of pathological cardiac

*To whom correspondence should be addressed: Michael S. Kapiloff, M.D., Ph.D., Stanford University, 1651 Page Mill Road, Room 2112, Palo Alto, CA 94304-1209, Phone: 650-724-0628, kapiloff@stanford.edu.

Author Contributions

ECM performed *in vivo* mouse research and analysis of primary data with the assistance of JL and HT. JAA performed human induced cardiomyocyte experiments. KT performed rat cardiomyocyte experiments. MSK, ECM, IK, and KDK wrote the paper. MSK provided overall supervision for the project.

Ethical Approval

Animal research was approved by the Institutional Animal Care and Use Committee at the University of Miami and the University of Connecticut. The Stanford University Institutional Review Board approved the use of pluripotent stem cells.

Competing Interests

Drs. Kapiloff and Li are inventors of patent-protected intellectual property concerning the targeting of mAKAPβ signalosomes to treat heart failure, by which they, the University of Miami, and Stanford University may gain royalties from future commercialization. Dr. Kapiloff holds equity in Anchored RSK3 Inhibitors, LLC, and Cardiac RSK3 Inhibitors, LLC, companies interested in developing mAKAP signalosome-targeted therapies.

remodeling and heart failure, providing long-term restoration of left ventricular ejection fraction. Our findings provide proof-of-concept for mAKAPβ as a therapeutic target for ischemic cardiomyopathy and support the development of a translational pipeline for AAV9sc.shmAKAP for the treatment of heart failure.

Introduction

Coronary heart disease is a major cause of morbidity and mortality worldwide, as well as a major risk factor for heart failure (1). Heart failure after myocardial infarction (MI) is a consequence of pathological remodeling that occurs in both the infarcted and remote areas of the myocardium. The high mortality associated with heart failure (~50% survival five years after diagnosis) underscores an unmet need for more effective anti-remodeling therapies beyond those therapies currently prescribed for ischemic cardiomyopathy (2).

Altered cardiomyocyte function is a major contributor to pathological cardiac remodeling, that at the molecular level is regulated by a network of intracellular signaling pathways controlling different aspects of remodeling, including myocyte hypertrophy, apoptosis, and autophagy, altered myocyte metabolism and contractility, and myocardial inflammation and fibrosis (3). While it is possible to target therapeutically individual signaling proteins such as plasmalemmal receptors or key signaling intermediates, we and others have proposed that an alternative approach is to target multimolecular signaling complexes or “signalosomes” that comprise nodes within signaling networks (4, 5). Signalosomes are compartmentalized multi-protein complexes organized by scaffold proteins that bind together components of different signaling pathways, facilitating pathway crosstalk and conferring the specific regulation of cellular processes (6). Targeting signalosome function by inhibiting either scaffold protein expression or blocking the recruitment of individual signalosome components can be an effective approach to inhibit or reverse a pathological process (7–9). Notably, the advent of adeno-associated virus (AAV) gene therapy vectors that can effectively deliver a small hairpin RNA (shRNA) or competing binding peptide to cell types of interest provides an opportunity to develop new therapeutics for heart failure distinct from conventional plasmalemmal receptor antagonists or enzyme active site inhibitors (10).

In cardiomyocytes, perinuclear signalosomes organized by the 230 kDa scaffold mAKAPβ regulate gene expression in response to diverse upstream stimuli, including cAMP, Ca^{2+}, phosphatidylinositol, mitogen-activated protein kinase, and hypoxic signaling (Supplementary Figure 1) (11). At mAKAPβ signalosomes, nuclear factor of activated T-cells (NFATc), myocyte enhancer factor (MEF2), serum response factor (SRF), and hypoxia-inducible factor 1-α (HIF-1α) transcription factors and class IIa histone deacetylases are post-translationally modified, modulating gene expression regulating pathological cardiac remodeling (7, 9, 12–15). Accordingly, myocyte-specific *mAKAP* gene deletion attenuated cardiac hypertrophy in a mouse model of chronic pressure overload, inhibiting myocyte cell death and myocardial fibrosis, while preventing heart failure and improving survival (9). Here, we demonstrate that targeting of mAKAPβ signalosomes via inhibited scaffold expression is beneficial in ischemic cardiomyopathy. We describe a new self-complementary

AAV gene therapy vector expressing an shRNA for mAKAP (AAV9sc.shmAKAP) that is efficacious in preventing pathological cardiac remodeling and heart failure in the setting of MI in mice. Taken together, the data presented herein provide the premise for a new translational pipeline for the treatment of heart failure that may be efficacious across diverse cardiovascular diseases.

Materials and Methods

Animal Studies:

The *mAKAP* conditionally targeted mouse B6;SJL-*Akap6*$^{tm1.1Mskf}$/Mmjax (MMRRC stock 37540-Jax, "*mAKAP*^{fl}", The Jackson Laboratory, Bar Harbor, Maine) was previously described (9). Conditional cardiomyocyte-specific knock-out was achieved by mating *mAKAP*^{fl} and Tg(Myh6-Cre/Esr1*)1Jmk/J mice ("MCM", strain 005657, The Jackson Laboratory) (16). For gene therapy studies, AAV was injected intravenously (5×10^{11} vg i.v.) via the tail vein into adult wildtype C57BL/6 mice of mixed N and J lineage bred in-house. Both male and female mice were included in all cohorts. Although formal power analyses were not performed prior to the MI studies shown here, cohort size was similar to prior studies (7). Masking of animal cohorts was not performed.

Design of AAV9sc.shmAKAP:

The pscA-TnT-mAKAP and control shRNA shuttle plasmids included as follows: the chicken cardiac troponin T promoter that confers cardiomyocyte-specific expression (17); a human *MIR30A* shRNA cassette designed as previously described (18); and an SV40-derived polyadenylation sequence (SV40 genome bp 2599–2769). The shRNA mini-genes were flanked by AAV2 ITR sequences (NC_001401.2 bp 4489–4664 in antisense orientation at the 5' end and bp 4559–4662 at the 3' end) to direct production of a self-complementary AAV (AAVsc) vector (19). The *mAKAP* target sequence was GGAGGAAATAGCAAGGTTA (bp 7915–7933 in the 3' non-coding region of NCBI reference sequence NM_004274). The control shRNA sequence was ACAGTCCGTACTGGAGAGATGC. AAV9sc.shmAKAP and AAV9sc.shControl were generated by the University of Pennsylvania Vector Core. AAV2sc shRNA viruses for infection of induced cardiomyocytes (iPSC-CMs) were generated using similar shuttle plasmids that contained a cytomegalovirus immediate early promoter (CMVie). Complete sequences of the AAV species are available upon request. Adenoviruses expressing an mAKAP (targeting bp 7210–7228, GI:5070430) or control shRNA were previously described (20).

Ligation of the Left Coronary Artery:

MI was induced under isoflurane anesthesia and oro-tracheal intubation as previously described (7). Briefly, following pericardiectomy, the left coronary artery was permanently ligated with a suture to produce an antero-apical MI. Sham-operated mice that experienced all but the placement of the coronary artery ligature served as non-infarcted controls. Mortality in this study was ~20% regardless of mouse genotype and limited to the intra- or peri-operative period (within a day of surgery). Echocardiography and histochemistry were performed as previously described (7). For the AAV study, infarcted mice were included

only if LV fractional shortening was less than 20% as assessed by echocardiography 2 days post-infarction. Sham-operated and infarcted mice were randomized into two AAV-treated cohorts each using the online GraphPad Quickcalcs randomizing tool.

Western blotting:

Protein lysates from whole heart tissue were analyzed by western blot using custom-made rabbit anti-mAKAP antibodies (VO54) as previously described (21).

Adult rat ventricular myocyte isolation and culture:

Ventricular myocytes were isolated from 2–3-month-old Sprague-Dawley rats and infected with mAKAP and control shRNA adenovirus (MOI = 50), as previously described (7, 20). After stimulation with isoproterenol (Iso, 1 μM) for 2 days, TdT-mediated dUTP Nick-end Labeling (TUNEL) staining (DeadEnd Fluorometric TUNEL System, Promega, Madison, Wisconsin) was performed as described by the manufacturer.

iPSC CM differentiation and AAV infection.

Human iPSCs derived from three different healthy donors and provided by the Stanford CVI iPSC biobank (lines SCVI-15, SCVI 273 and SCVI-274) were maintained and differentiated towards cardiomyocytes using established protocols (22). At 45 days post-differentiation, iPSC-CMs were seeded in 12-well plates coated with Geltrex (Thermofisher, Waltham, Massachusetts) at a density of 5×10^5 cells/well, infected with AAV2sc.shmAKAP or AAV2sc.shControl viruses (10^3 vg per cell), and cultured for 1 week before protein expression analysis.

Statistical Analysis:

Statistics were computed using Prism 9 (Graphpad, San Diego, California). *n* refers to the number of individual mice or myocyte preparations. All data are expressed as mean ± s.e.m. Two-way ANOVA was performed for experiments involving two-way design. *p*-values for experiments involving multiple comparisons were obtained by Tukey test.

Results

mAKAPβ facilitates adult rat ventricular myocyte death in response to β-adrenergic stimulation

We have previously reported that conditional, cardiomyocyte-specific mAKAPβ gene deletion (mAKAP CKO) attenuated the pathological cardiac remodeling and heart failure induced by long-term pressure overload, including cardiac hypertrophy, interstitial myocardial fibrosis, and increased myocyte death (9). mAKAPβ signalosomes have generally been associated with the regulation of cardiomyocyte hypertrophy (11). Given the decreased myocyte death in mAKAP CKO mice subjected to long-term pressure overload, we considered that mAKAPβ-dependent signaling might promote cardiomyocyte death in a cell-autonomous manner. Primary adult rat ventricular myocytes *in vitro* were infected with adenovirus that expresses either an mAKAP or control shRNA (20). Depletion of mAKAPβ did not affect the survival of myocytes cultured in a minimal medium (Figure 1), similar to

the lack of overt phenotype for unstressed mAKAP CKO mice (9). Notably, the expression of mAKAP shRNA blocked the excess cell death induced by stimulation for two days with the β-adrenergic agonist isoproterenol (Iso, 10 μmol/L).

Condition *mAKAP* gene deletion prevents cardiac remodeling following myocardial infarction

As mAKAPβ depletion inhibited cardiomyocyte death *in vitro*, we considered that mAKAPβ targeting would also benefit ischemic heart disease, in which myocyte loss is prominent. As previously described (9), mAKAP CKO was induced in $mAKAP^{fl/fl}$; Tg(Myh6-Cre/Esr1*) mice at eight weeks of age by provision of oral tamoxifen for 1 week. MI was subsequently induced by permanent ligation of the left coronary artery at ten weeks of age. Control cohorts included tamoxifen-treated $mAKAP^{f/f}$ and Tg(Myh6-Cre/Esr1*) "MCM" mice to account for any effects of loxP site insertion and expression of the tamoxifen-inducible Cre recombinase protein, respectively. Consistent with our previous observations (9), mAKAP CKO showed no significant phenotype in sham-operated, un-stressed mice. By echocardiography, 4 weeks post-MI, the control cohorts showed decreased motility of the left ventricular (LV) anterior wall consistent with an infarction in that part of the heart (Figure 2a). In addition, the control cohorts showed prominent LV dilatation and decreased systolic function as evidenced by increased diastolic and systolic LV internal diameters and volumes and decreased LV fractional shortening and ejection fraction (Figure 2b-d, Table 1).

In contrast, mAKAP CKO mice exhibited preserved LV anterior wall mobility and thickening with contraction in systole (Figure 2a,e, Table 1). Accordingly, mAKAP CKO mice had preserved LV dimensions and systolic function. While overall ventricular hypertrophy and heart failure (as indicated by increased wet lung weight) was not consistently detected in the control cohorts 4 weeks post-MI, gravimetric analysis showed that infarcted control mice, but not infarcted mAKAP CKO mice exhibited atrial hypertrophy, a marker of the diastolic dysfunction typically a consequence of advanced LV systolic dysfunction (Table 1). Taken together, these results showed that mAKAPβ expression was required for the deterioration in cardiac function following myocardial infarction, implying that mAKAPβ targeting might be a rational approach to the prevention of post-MI pathological cardiac remodeling.

A new gene therapy vector targeting mAKAPβ

To develop a clinically applicable gene therapy inhibiting mAKAPβ-dependent pathological remodeling, we identified a conserved mRNA sequence that might be targeted by RNA interference (Figure 3a). Self-complementary serotype 9 adeno-associated virus (AAV9sc) were constructed in which *MIR30A* shRNA cassettes for the mAKAP or a control sequence were expressed under the direction of the cardiomyocyte-specific chicken troponin T promoter, namely AAV9sc.shmAKAP and control AAV9sc.shControl (17). AAV9sc.shmAKAP administration resulted in ~80% reduction in cardiac mAKAPβ protein in adult mice (Figure 3c). AAV-mediated expression of the mAKAP shRNA also inhibited mAKAPβ expression in human induced pluripotent stem cell-derived cardiomyocytes

(iPSC-CMs, Figure 3d), demonstrating that mAKAPβ mRNA might be targeted in human patients using the same shRNA construct.

Prevention of post-infarction cardiac remodeling by AAV9sc.shmAKAP

To obtain proof-of-concept that mAKAPβ targeting would prevent pathological cardiac remodeling following MI, 8–10 week-old wildtype C57BL/6 mice were subjected to permanent ligation of the left coronary artery or sham survival surgery (Figure 4a). Two days after surgery, the infarcted and sham-operated mice were randomized into two groups each with similar LV fractional shortening (Table 2). The third day after surgery, infarcted and sham-operated mice were treated with either AAV9sc.shMAKAP or AAV9sc.shControl virus. Similar to infarcted MCM and *mAKAP*$^{f/f}$ mice (Figure 2), AAV9sc.shControl-injected infarcted mice exhibited a progressive decline in LV systolic function as measured by fractional shortening and ejection fraction and LV dilatation in both systole and diastole Figure 4c-e and Table 2). AAV9sc.shMAKAP treatment resulted in a rapid and persistent improvement in cardiac structure and function for infarcted mice compared to AAV9sc.shControl treatment. mAKAPβ targeting resulted in preserved anterior wall thickening and motility (Figure 4b and Table 2), and significant improvement in LV volumes in diastole and systole (Figure 4c,d and Table 2). Notably, AAV9sc.shmAKAP resulted in a persistent restoration of contractility following MI as indicated by ejection fraction and fractional shortening (Figure 4e and Table 2).

Post-MI, the improvement in echocardiographic parameters due to AAV9sc.shmAKAP treatment correlated with a significant decrease in biventricular hypertrophy (Figure 4f). While the improvement in atrial hypertrophy did not quite reach statistical significance (Figure 4g), wet lung weight, an assay for pulmonary edema and a marker for heart failure, was significantly less after MI for AAV9sc.shmAKAP-treated mice and was similar to that for the sham-operated cohorts (Figure 4h). Gross inspection of the infarcted hearts post-mortem showed a noticeable improvement in overall heart and infarct size following AAV9sc.shmAKAP-treatment (Figure 4i). Accordingly, the infarct area measured in Masson Trichrome-stained transverse sections was 49% less in treated mice (Figure 4j,k). Finally, western blot analysis of remote wall samples confirmed the efficient inhibition of mAKAPβ expression by AAV9sc.shmAKAP transduction (Supplementary Figure 2), while revealing that despite the function of the mAKAPβ scaffold in organizing signalosomes promoting pathological remodeling, expression of mAKAPβ itself was not altered following infarction (expression in AAV9sc.shControl-injected tissue). Together, these results show that treatment with a self-complementary AAV gene therapy vector targeting cardiomyocyte mAKAPβ expression provided significant improvement in cardiac structure and function after MI, preventing the development of heart failure.

Discussion

In this study, we show that the perinuclear scaffold protein mAKAPβ is required for pathological cardiac remodeling following MI. We demonstrate that inhibition of cardiomyocyte mAKAPβ expression, whether by *mAKAP* gene targeting or by treatment with the new AAV9sc.shmAKAP gene therapy vector, preserves cardiac structure and

function and prevents heart failure in a murine model of ischemic cardiomyopathy. In conjunction with previous studies (9, 11), our findings support a new gene therapy translational pipeline targeting mAKAPβ expression in ischemic heart disease and other common diseases such as hypertension or aortic stenosis.

This study provides proof-of-concept for a new gene therapy for heart failure. The strategy for mAKAPβ targeting is based upon AAV9-mediated gene delivery to the heart of an shRNA mini-gene. AAV9-based biologics have become common in clinical trials since the approval of onasemnogene abeparvovec (Zolgensma) for spinal muscular atrophy in the USA in 2019 (23). Although AAV9 targets other organs, including liver and skeletal muscle, it is currently the most frequently used AAV serotype for targeting the heart, as it transduces cardiomyocytes with high efficiency (10), especially after ischemic events (24). The *mAKAP* gene is expressed primarily in striated muscle and neurons (21), and to a lesser degree in other cell types such as osteoclasts (25). Using the cardiomyocyte-specific cardiac troponin T promoter, AAV9sc.shmAKAP restricts the expression of the mAKAP shRNA in the heart, minimizing off-target effects (17). The shRNA target sequence in AAV9sc.shmAKAP is conserved across mammalian species, and interference with mAKAPβ expression in human iPSC-CMs supports its potential utility in human disease. While alternative approaches to inhibit mAKAPβ expression could be designed, including CRISPR-mediated gene targeting or CRISPRi-mediated gene repression (26), the efficacy of the current shRNA vector provides an immediate strategy for targeting mAKAPβ in disease.

Following the immediate loss of cardiomyocytes by necrosis and apoptosis, initial remodeling post-MI involves inflammation, cellular debris resorption, and extracellular matrix remodeling contributing to wound healing and infarct expansion (27–29). In addition to reparative fibrosis and mature scar formation, subsequent remodeling includes changes in the surviving myocardium, including myocyte hypertrophy and apoptosis, reactive fibrosis, recruitment of border zone myocardium into the scar, and progressive chamber dilatation (30). The mechanisms by which AAV9sc.shmAKAP might be beneficial in ischemic cardiomyopathy are multiple. Here we show that mAKAPβ depletion improved the survival of stressed cultured adult cardiomyocytes in a cell-autonomous manner. In the AAV9sc.shmAKAP treatment study, the biologic drug was administered three days after infarction. In this case, the beneficial effects of inhibiting apoptosis were likely to be most important for preventing myocyte loss in the later phases of post-MI remodeling when apoptosis is associated with LV dysfunction and worse patient outcome (30, 31). Notably, conditional *mAKAP* gene targeting prior to MI was also beneficial, implying that loss of mAKAPβ expression prior to an ischemic event will not exacerbate the outcome. This observation is important as other potential drug targets candidates for heart failure like calcineurin Aβ and the mitogen-activated protein kinase ERK1/2 are required for not only pathological cardiac remodeling, but also myocyte survival, such that there is increased loss of myocardium during ischemia when these enzymes are targeted (32, 33). In contrast, loss of mAKAPβ appears to protect adult cardiomyocytes from cell death both *in vitro* and in disease models (9).

In addition to preventing myocyte cell loss, AAV9sc.shmAKAP treatment following an infarction should inhibit pathological cardiomyocyte hypertrophy contributing to ventricular

dilatation and worsening cardiac dysfunction (29). By organizing signalosomes that control critical gene regulatory pathways, mAKAPβ serves as a node in the myocyte pathological remodeling signaling network (Supplementary Figure 1). NFATc2 and NFATc3 transcription factors are required to induce pathological cardiac hypertrophy (34, 35), and mAKAPβ is necessary for the calcineurin-dependent nuclear translocation and activation of NFATc transcription factors in cardiomyocytes (13, 20). In addition, MEF2D is required for pathological cardiac remodeling (36), and mAKAPβ is necessary for the calcineurin-dependent switch in MEF2D binding from class IIa histone deacetylase to p300 histone acetylase associated with increased MEF2D-dependent gene expression (37). Further, mAKAPβ is required for the protein kinase D-dependent nuclear export of class IIa histone deacetylases that is critical for pathological myocyte hypertrophy (14, 38). Finally, mAKAPβ is proposed to facilitate protein kinase A-dependent PP2A dephosphorylation of SRF, promoting eccentric cardiac hypertrophy following MI (7, 39). Thus, by targeting mAKAPβ and inhibiting the multiple pathological gene regulatory pathways controlled by mAKAPβ signalosomes, AAV9sc.shmAKAP can block pathological remodeling and preserve cardiac function in ischemic heart disease, as well as presumably in other prevalent acquired cardiac diseases. The anticipated efficacy of AAV9sc.shmAKAP in disease is in contrast to the expectation that targeting cardiac mAKAPβ will not affect the function of normal cardiomyocytes. As confirmed for the sham-operated mice, loss of mAKAPβ apparently has no significant deleterious effects in the healthy heart, whether induced during development or in the adult (9).

mAKAPβ is an example of a compartmentalized scaffold protein whose expression is highly localized within the cell, in this case by binding to the integral membrane protein nesprin-1α that is on the nuclear envelope (40). The lack of deleterious baseline phenotype of the mAKAP CKO mouse is consistent with mAKAPβ being a relatively low abundant protein whose function is dedicated to the regulation of stress-induced cardiomyocyte gene expression (11). While promising, the study of mAKAPβ has thus far been restricted to small rodent model systems. Facilitated by the conservation of the AAV9sc.shmAKAP mAKAPβ mRNA target sequence in swine, the next step in the translational pipeline for AAV9sc.shmAKAP will be to test the efficacy of this biologic in a large animal model of cardiovascular disease (41). Evidence that AAV9sc.shmAKAP is protective following MI in swine will confirm mAKAPβ relevance to cardiomyocyte regulation across mammalian species and justify first-in-human clinical trials.

Supplementary Material

Refer to Web version on PubMed Central for supplementary material.

Funding

This work was supported by NIH Grants R01HL126825, R01HL153835, and R01HL146111 (Dr. Kapiloff and Dr. Dodge-Kafka) and the NHLBI Gene Therapy Resource Program.

Data Availability

Additional data and original echocardiographic images are available from the corresponding author on reasonable request.

References

1. Virani SS, Alonso A, Aparicio HJ, Benjamin EJ, Bittencourt MS, Callaway CW, et al. Heart Disease and Stroke Statistics-2021 Update: A Report From the American Heart Association. Circulation 2021;143(8):e254–e743. [PubMed: 33501848]
2. McDonagh TA, Metra M, Adamo M, Gardner RS, Baumbach A, Bohm M, et al. 2021 ESC Guidelines for the diagnosis and treatment of acute and chronic heart failure. Eur Heart J 2021;42(36):3599–726. [PubMed: 34447992]
3. Nakamura M, Sadoshima J. Mechanisms of physiological and pathological cardiac hypertrophy. Nature reviews Cardiology 2018;15(7):387–407. [PubMed: 29674714]
4. Omar MH, Scott JD. AKAP Signaling Islands: Venues for Precision Pharmacology. Trends Pharmacol Sci 2020;41(12):933–46. [PubMed: 33082006]
5. Negro A, Dodge-Kafka K, Kapiloff MS. Signalosomes as Therapeutic Targets. Prog Pediatr Cardiol 2008;25(1):51–6. [PubMed: 19343079]
6. Zaccolo M, Zerio A, Lobo MJ. Subcellular Organization of the cAMP Signaling Pathway. Pharmacol Rev 2021;73(1):278–309. [PubMed: 33334857]
7. Li J, Tan Y, Passariello CL, Martinez EC, Kritzer MD, Li X, et al. Signalosome-Regulated Serum Response Factor Phosphorylation Determining Myocyte Growth in Width Versus Length as a Therapeutic Target for Heart Failure. Circulation 2020;142(22):2138–54. [PubMed: 32933333]
8. Li X, Li J, Martinez EC, Froese A, Passariello CL, Henshaw K, et al. Calcineurin Abeta-Specific Anchoring Confers Isoform-Specific Compartmentation and Function in Pathological Cardiac Myocyte Hypertrophy. Circulation 2020;142(10):948–62. [PubMed: 32611257]
9. Kritzer MD, Li J, Passariello CL, Gayanilo M, Thakur H, Dayan J, et al. The scaffold protein muscle A-kinase anchoring protein beta orchestrates cardiac myocyte hypertrophic signaling required for the development of heart failure. Circulation Heart failure 2014;7(4):663–72. [PubMed: 24812305]
10. Kieserman JM, Myers VD, Dubey P, Cheung JY, Feldman AM. Current Landscape of Heart Failure Gene Therapy. J Am Heart Assoc 2019;8(10):e012239. [PubMed: 31070089]
11. Dodge-Kafka K, Gildart M, Tokarski K, Kapiloff MS. mAKAPbeta signalosomes - A nodal regulator of gene transcription associated with pathological cardiac remodeling. Cell Signal 2019;63:109357. [PubMed: 31299211]
12. Li J, Vargas MA, Kapiloff MS, Dodge-Kafka KL. Regulation of MEF2 transcriptional activity by calcineurin/mAKAP complexes. Exp Cell Res 2013;319(4):447–54. [PubMed: 23261540]
13. Li J, Negro A, Lopez J, Bauman AL, Henson E, Dodge-Kafka K, et al. The mAKAPbeta scaffold regulates cardiac myocyte hypertrophy via recruitment of activated calcineurin. J Mol Cell Cardiol 2010;48(2):387–94. [PubMed: 19883655]
14. Dodge-Kafka KL, Gildart M, Li J, Thakur H, Kapiloff MS. Bidirectional regulation of HDAC5 by mAKAPbeta signalosomes in cardiac myocytes. J Mol Cell Cardiol 2018;118:13–25. [PubMed: 29522762]
15. Wong W, Goehring AS, Kapiloff MS, Langeberg LK, Scott JD. mAKAP compartmentalizes oxygen-dependent control of HIF-1alpha. Sci Signal 2008;1(51):ra18. [PubMed: 19109240]
16. Sohal DS, Nghiem M, Crackower MA, Witt SA, Kimball TR, Tymitz KM, et al. Temporally regulated and tissue-specific gene manipulations in the adult and embryonic heart using a tamoxifen-inducible Cre protein. Circ Res 2001;89(1):20–5. [PubMed: 11440973]
17. Prasad KM, Xu Y, Yang Z, Acton ST, French BA. Robust cardiomyocyte-specific gene expression following systemic injection of AAV: in vivo gene delivery follows a Poisson distribution. Gene Ther 2011;18(1):43–52. [PubMed: 20703310]

18. Silva JM, Li MZ, Chang K, Ge W, Golding MC, Rickles RJ, et al. Second-generation shRNA libraries covering the mouse and human genomes. Nat Genet 2005;37(11):1281–8. [PubMed: 16200065]
19. Wang Z, Ma HI, Li J, Sun L, Zhang J, Xiao X. Rapid and highly efficient transduction by double-stranded adeno-associated virus vectors in vitro and in vivo. Gene Ther 2003;10(26):2105–11. [PubMed: 14625564]
20. Pare GC, Bauman AL, McHenry M, Michel JJ, Dodge-Kafka KL, Kapiloff MS. The mAKAP complex participates in the induction of cardiac myocyte hypertrophy by adrenergic receptor signaling. J Cell Sci 2005;118(Pt 23):5637–46. [PubMed: 16306226]
21. Kapiloff MS, Schillace RV, Westphal AM, Scott JD. mAKAP: an A-kinase anchoring protein targeted to the nuclear membrane of differentiated myocytes. J Cell Sci 1999;112 (Pt 16):2725–36. [PubMed: 10413680]
22. Feyen DAM, Perea-Gil I, Maas RGC, Harakalova M, Gavidia AA, Arthur Ataam J, et al. Unfolded Protein Response as a Compensatory Mechanism and Potential Therapeutic Target in PLN R14del Cardiomyopathy. Circulation 2021;144(5):382–92. [PubMed: 33928785]
23. Kuzmin DA, Shutova MV, Johnston NR, Smith OP, Fedorin VV, Kukushkin YS, et al. The clinical landscape for AAV gene therapies. Nat Rev Drug Discov 2021;20(3):173–4. [PubMed: 33495615]
24. Konkalmatt PR, Wang F, Piras BA, Xu Y, O'Connor DM, Beyers RJ, et al. Adeno-associated virus serotype 9 administered systemically after reperfusion preferentially targets cardiomyocytes in the infarct border zone with pharmacodynamics suitable for the attenuation of left ventricular remodeling. The journal of gene medicine 2012;14(9–10):609–20. [PubMed: 23065925]
25. Vergarajauregui S, Becker R, Steffen U, Sharkova M, Esser T, Petzold J, et al. AKAP6 orchestrates the nuclear envelope microtubule-organizing center by linking golgi and nucleus via AKAP9. Elife 2020;9.
26. Wang D, Zhang F, Gao G. CRISPR-Based Therapeutic Genome Editing: Strategies and In Vivo Delivery by AAV Vectors. Cell 2020;181(1):136–50. [PubMed: 32243786]
27. Fraccarollo D, Galuppo P, Bauersachs J. Novel therapeutic approaches to post-infarction remodelling. Cardiovasc Res 2012;94(2):293–303. [PubMed: 22387461]
28. Frangogiannis NG. Pathophysiology of Myocardial Infarction. Compr Physiol 2015;5(4):1841–75. [PubMed: 26426469]
29. Sutton MG, Sharpe N. Left ventricular remodeling after myocardial infarction: pathophysiology and therapy. Circulation 2000;101(25):2981–8. [PubMed: 10869273]
30. Sam F, Sawyer DB, Chang DL, Eberli FR, Ngoy S, Jain M, et al. Progressive left ventricular remodeling and apoptosis late after myocardial infarction in mouse heart. Am J Physiol Heart Circ Physiol 2000;279(1):H422–8. [PubMed: 10899082]
31. Abbate A, Biondi-Zoccai GG, Bussani R, Dobrina A, Camilot D, Feroce F, et al. Increased myocardial apoptosis in patients with unfavorable left ventricular remodeling and early symptomatic post-infarction heart failure. J Am Coll Cardiol 2003;41(5):753–60. [PubMed: 12628718]
32. Bueno OF, Lips DJ, Kaiser RA, Wilkins BJ, Dai YS, Glascock BJ, et al. Calcineurin Abeta gene targeting predisposes the myocardium to acute ischemia-induced apoptosis and dysfunction. Circ Res 2004;94(1):91–9. [PubMed: 14615291]
33. Lips DJ, Bueno OF, Wilkins BJ, Purcell NH, Kaiser RA, Lorenz JN, et al. MEK1-ERK2 signaling pathway protects myocardium from ischemic injury in vivo. Circulation 2004;109(16):1938–41. [PubMed: 15096454]
34. Bourajjaj M, Armand AS, da Costa Martins PA, Weijts B, van der Nagel R, Heeneman S, et al. NFATc2 is a necessary mediator of calcineurin-dependent cardiac hypertrophy and heart failure. J Biol Chem 2008;283(32):22295–303. [PubMed: 18477567]
35. Wilkins BJ, De Windt LJ, Bueno OF, Braz JC, Glascock BJ, Kimball TF, et al. Targeted disruption of NFATc3, but not NFATc4, reveals an intrinsic defect in calcineurin-mediated cardiac hypertrophic growth. Mol Cell Biol 2002;22(21):7603–13. [PubMed: 12370307]
36. Kim Y, Phan D, van Rooij E, Wang DZ, McAnally J, Qi X, et al. The MEF2D transcription factor mediates stress-dependent cardiac remodeling in mice. J Clin Invest 2008;118(1):124–32. [PubMed: 18079970]

37. Li J, Aponte Paris S, Thakur H, Kapiloff MS, Dodge-Kafka KL. Muscle A-kinase-anchoring protein-beta-bound calcineurin toggles active and repressive transcriptional complexes of myocyte enhancer factor 2D. J Biol Chem 2019;294(7):2543–54. [PubMed: 30523159]

38. Zhang L, Malik S, Pang J, Wang H, Park KM, Yule DI, et al. Phospholipase Cepsilon hydrolyzes perinuclear phosphatidylinositol 4-phosphate to regulate cardiac hypertrophy. Cell 2013;153(1):216–27. [PubMed: 23540699]

39. Dodge-Kafka KL, Bauman A, Mayer N, Henson E, Heredia L, Ahn J, et al. cAMP-stimulated protein phosphatase 2A activity associated with muscle A kinase-anchoring protein (mAKAP) signaling complexes inhibits the phosphorylation and activity of the cAMP-specific phosphodiesterase PDE4D3. J Biol Chem 2010;285(15):11078–86. [PubMed: 20106966]

40. Pare GC, Easlick JL, Mislow JM, McNally EM, Kapiloff MS. Nesprin-1alpha contributes to the targeting of mAKAP to the cardiac myocyte nuclear envelope. Exp Cell Res 2005;303(2):388–99. [PubMed: 15652351]

41. Dixon JA, Spinale FG. Large animal models of heart failure: a critical link in the translation of basic science to clinical practice. Circulation Heart failure 2009;2(3):262–71. [PubMed: 19808348]

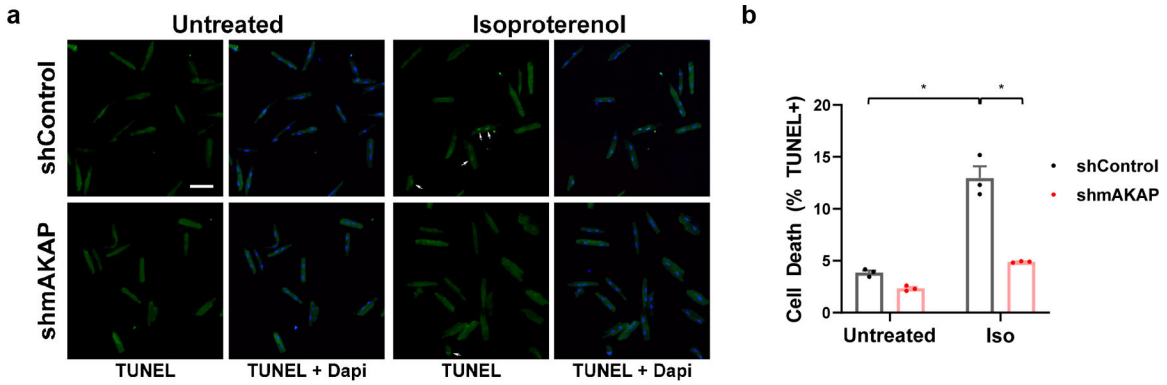

Figure 1. Targeting of mAKAPβ protects against isoproterenol-induced cardiomyocyte death *in vitro*.

a. Primary adult Sprague-Dawley rat ventricular myocytes were infected with adenovirus expressing mAKAP (shmAKAP) or control shRNA (shControl) and cultured in minimal medium for two days with and without 10 μmol/L isoproterenol (Iso) before TUNEL staining. TUNEL - green; Dapi nuclear stain – blue; bar - 100 μm. Arrowheads indicate nuclei with detectable TUNEL labeling. **b.** Quantification of TUNEL-positive cells (mean ± s.e.m.) for 3 independent experiments. * $p < 0.05$.

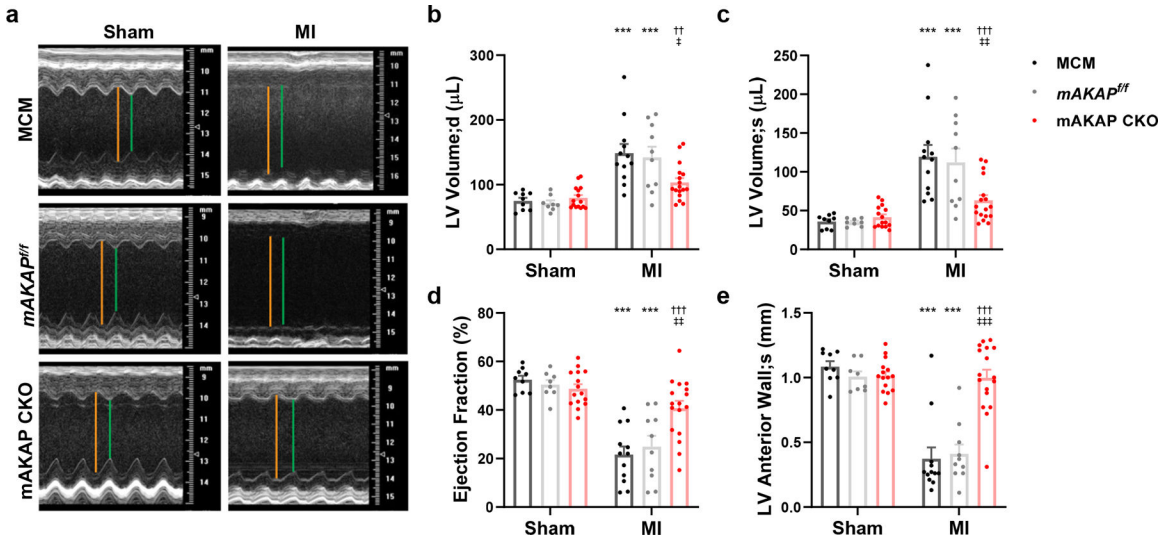

Figure 2. Cardiomyocyte-specific mAKAPβ knock-out prevents systolic dysfunction following myocardial infarction.

Following oral administration of tamoxifen (125 mg/kg chow) for one week starting at 8 weeks of age to induce gene knock-out, mAKAP CKO mice and control *mAKAP*$^{f/f}$ and MCM mice underwent permanent ligation of the left coronary artery survival surgery at ten weeks of age or sham operation. M-mode echocardiography was performed 4 weeks post-MI. **a.** Representative echocardiographic images. Left ventricular internal diameter indicated in diastole (LVID;d - orange) and systole (LVID;s - green). **b-e.** Left ventricular volume in diastole (b) and systole (c), ejection fraction (d), and anterior wall thickness in systole (e). Bars show mean ± s.e.m. Data were analyzed by two-way ANOVA with Tukey post-hoc testing. *n*: MCM-sham - 9; *mAKAP*$^{f/f}$-sham - 8; mAKAP CKO-sham – 15; MCM-MI- 12; *mAKAP*$^{f/f}$-MI - 10; mAKAP CKO-MI – 17. * vs. sham for the same genotype; † vs. MCM-MI; ‡ vs. *mAKAP*$^{f/f}$-MI. ‡ $p < 0.05$; ††,‡‡ $p < 0.01$; ***,†††,‡‡‡ $p < 0.001$. There were no significant differences among the 3 sham-operated cohorts.

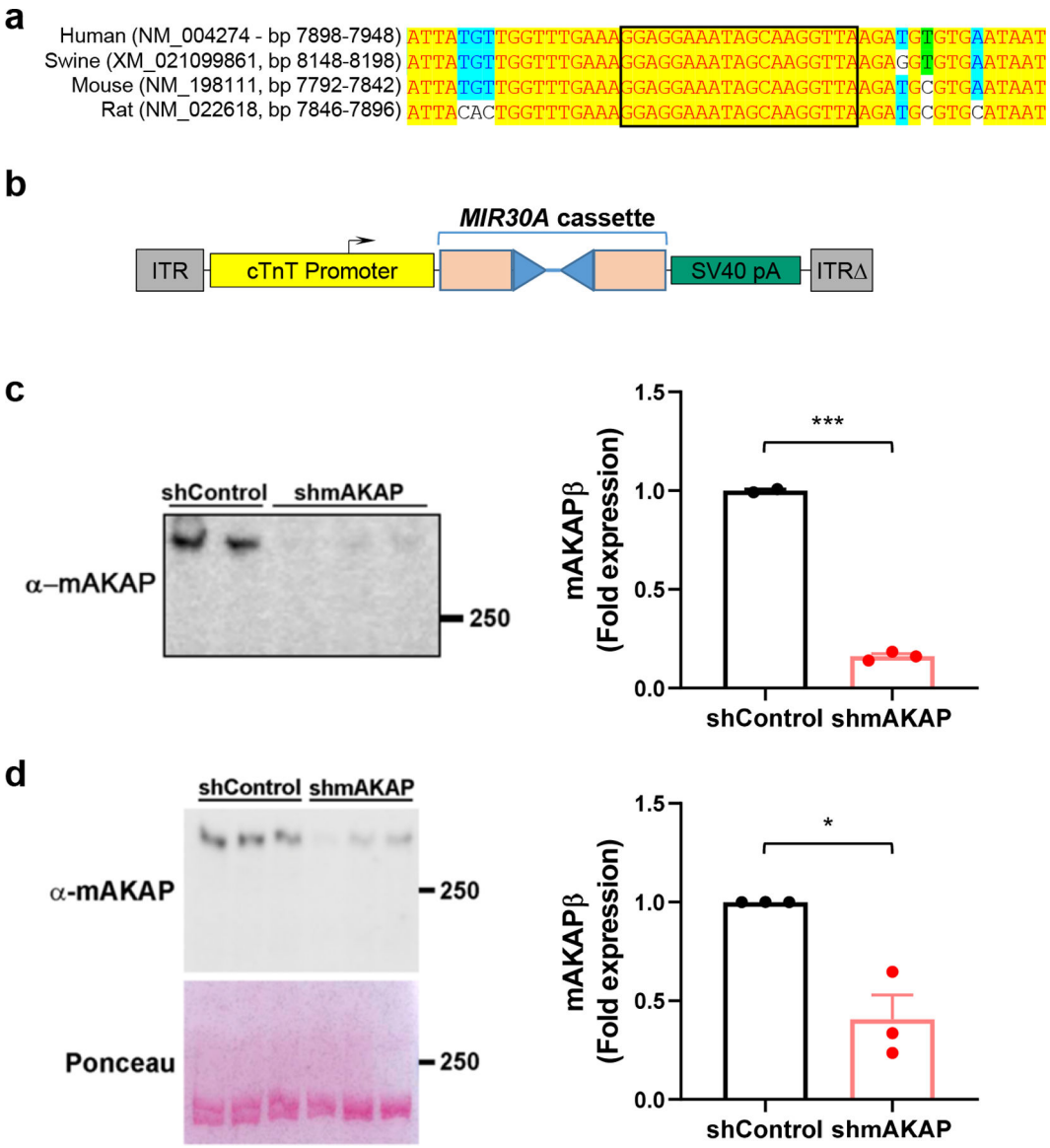

Figure 3. A new shRNA gene therapy vector inhibits mAKAPβ expression.

a. Alignment of mAKAP mRNA sequences from different vertebrate species. Conserved mAKAP shRNA target is in box. **b.** Design of an AAV9sc shRNA vector. ITR – AAV inverted terminal repeat (intact and deleted "Δ"); cTnT – chicken cardiac troponin T; beige blocks – human *MIR30A* genomic sequence; blue arrowheads – shRNA sequences. **c.** Western blot for mAKAPβ in whole heart extracts from individual adult mice 3 weeks after tail vein intravenous (IV) injection with 5×10^{11} viral genomes (vg) AAV9sc.shmAKAP (n = 3) or AAV9sc.shControl virus (n = 2). Graph shows mAKAPβ expression (mean ± s.e.m.) normalized to total protein detected by Ponceau stain of the same blot (not shown). *** $p <$ 0.001. See also Supplementary Figure 2. **d.** Normal human iPSC-CMs were infected 1 week before analysis by mAKAP western blot with AAV2sc vectors expressing the mAKAP and control *MIR30A* cassettes (as in b) under the control of the CMV promoter (multiplicity of infection = 1000). Representative blot shows technical replicates for single iPSC line. Graph

shows average mAKAPβ expression (mean ± s.e.m. for mAKAP expression normalized to total protein detected by Ponceau stain of the same blot) for biological replicates performed with 3 different iPSC lines. * $p < 0.05$.

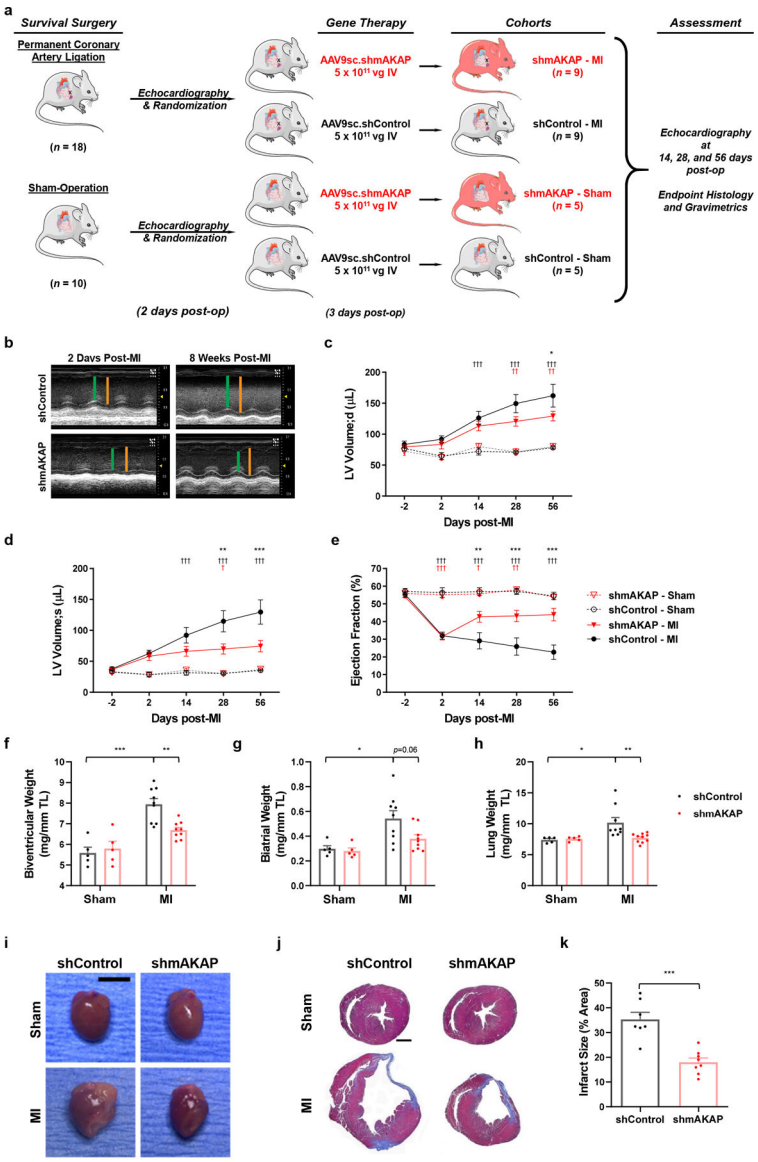

Figure 4. AAV9sc.shmAKAP treatment attenuates systolic dysfunction and prevents heart failure following myocardial infarction in mice.

a. Schema for AAV9sc.shmAKAP treatment study. C57BL/6 male and female mice were subjected at 8–10 weeks of age to permanent ligation of the left coronary artery or sham survival surgery. Echocardiographic data obtained 2 days after surgery was used to identify mice meeting inclusion criteria, followed by randomization to generate two groups each of sham-operated and infarcted mice. The 4 mouse cohorts were injected IV with 5×10^{11} vg of either AAV9sc.shmAKAP (highlighted in red) or AAV9sc.shControl the third day after survival surgery, followed by serial echocardiography and endpoint assessment 56 days post-operatively. This panel was drawn in part using pictures adapted from Servier Medical Art (http://smart.servier.com/), licensed under a Creative Commons Attribution 3.0 Unported License. **b.** Representative M-mode echocardiographic images. Left ventricular internal diameter indicated in diastole (LVID;d - orange) and systole (LVID;s - green). **c-e,** Left ventricular volume in diastole (c) and systole (d) and ejection fraction (e) by

serial M-mode echocardiography. shControl-sham – black circles; shControl-MI – black filled circles; shmAKAP-sham – red triangles; shmAKAP- MI – red filled triangles. * vs. shControl–MI; † vs. sham for same virus (color-coded). **f-h,** Biventricular, biatrial, and wet lung weights at endpoint normalized to tibial length (TL). *n* for panels c-h as indicated in panel a. **i,** Images of hearts at the endpoint. Bar – 5 mm. **j.** Masson Trichrome-stained transverse sections. Bar – 1 mm. **k.** Infarct area for MI heart sections at the level of the papillary muscles, measured in sections stained as in j. $n = 7,8$. *,† $p < 0.05$; **,†† $p < 0.01$; ***,††† $p < 0.001$.

Gene Ther. Author manuscript; available in PMC 2023 August 01.

Table 1:

mAKAP conditional knock-out mouse and myocardial infarction

		MCM - Sham	*mAKAP*$^{f/f}$ - Sham	mAKAP CKO -Sham	MCM - MI		*mAKAP*$^{f/f}$ - MI		mAKAP CKO - MI		
Echocardiography											
n		9	8	15	12		10		17		
LVPW;d	mm	0.72±0.03	0.71±0.02	0.70±0.02	0.69±0.07		0.61±0.05		0.74±0.04		
LVPW;s	mm	1.01±0.03	0.94±0.03	0.93±0.03	0.88±0.07		0.81±0.09		0.90±0.05		
LVAW;d	mm	0.74±0.03	0.71±0.04	0.69±0.04	0.29±0.06	***	0.37±0.05	***	0.72±0.04	†††	‡‡
LVAW;s	mm	1.08±0.04	1.01±0.04	1.01±0.03	0.37±0.09	***	0.41±0.07	***	1.00±0.06	†††	‡‡
LVID;d	mm	4.10±0.11	4.02±0.10	4.20±0.10	5.46±0.22	***	5.34±0.28	***	4.69±0.13	††	*a*
LVID;s	mm	3.01±0.10	2.99±0.06	3.18±0.11	4.93±0.26	***	4.75±0.35	***	3.76±0.16	†††	‡
LV Vol;d	μL	75±5	71±4	80±4	148±14	***	142±16	***	103±7	††	‡
LV Vol;s	μL	36±3	35±2	42±4	119±15	***	112±18	***	63±7	†††	‡
EF	%	52±2	50±2	49±2	22±3	***	25±4	***	41±3	†††	‡
FS	%	27±1	25±1	25±1	10±2	***	12±2	***	20±2	†††	‡
HR	BPM	494±8	496±15	519±8	504±15		479±14		507±7		
Gravimetrics											
n		8	10	18	15		13		17		
Body Weight	g	22.4±1.6	24.1±1.0	23.9±0.8	24.7±1.0		25.1±1.1		24.4±0.9		
Tibial Length	mm	17.8±0.2	18.0±0.1	18.1±0.1	17.9±0.1		18.0±0.1		17.9±0.1		
BiV/TL	mg/mm	5.4±0.2	6.2±0.2	5.8±0.2	7.2±0.3	**	7.3±0.4		6.8±0.2		
BiAW/TL	mg/mm	0.34±0.01	0.35±0.03	0.35±0.02	0.58±0.05	**	0.55±0.04	**	0.40±0.03	††	‡
LW/TL	mg/mm	7.4±0.3	7.4±0.3	7.8±0.2	9.7±0.9	*	8.0±0.2		7.6±0.2	††	

Mice were treated with tamoxifen at 8 weeks of age for 1 week and subjected to sham-operation or permanent left coronary artery ligation at 10 weeks of age, followed by analysis of surviving mice 4 weeks later. Mortality in this study was intra- or peri-operative (within a day of surgery) and ~20% regardless of mouse genotype. M-mode echocardiography parameters: LVPW, Left ventricular posterior wall thickness; LVAW, left ventricular anterior wall thickness; LVID, Left ventricular internal diameter; d, diastole; s, systole; Vol, Volume; EF, ejection fraction; FS, fractional shortening; BW, body weight; HR, heart rate. TL; tibial length; BiVW, biventricular weight; BiAW, biatrial weight; LW, lung weight. Data were analyzed by two-way ANOVA and Tukey post-hoc testing. All data are mean ± s.e.m.

$^{*}p$ vs. Sham-operated for same genotype;

$^{\dagger}p$ vs. MCM – MI;

‡p. vs. *mAKAP*$^{f/f}$ – MI.

$^{*,\dagger}p \leq 0.05$;

**,†† $p \leq 0.01$;

***,††† $p \leq 0.001$;

[a] $p = 0.06$ vs. *mAKAP*$^{f/f}$_ MI. There were no significant differences among the three sham-operated cohorts.

Gene Ther. Author manuscript; available in PMC 2023 August 01.

Table 2:

Treatment of myocardial infarction with AAV9sc.shmAKAP - Echocardiography

		shControl - Sham	shmAKAP - Sham	shControl - MI		shmAKAP - MI		
n		**5**	**5**	**9**		**9**		
2 Days Post-Infarction – Prior to AAV injection								
LVPW;d	mm	0.65±0.04	0.67±0.02	0.77±0.05		0.76±0.03		
LVPW;s	mm	0.97±0.04	0.97±0.06	0.96±0.05		0.91±0.04		
LVAW;d	mm	0.68±0.02	0.73±0.04	0.72±0.03		0.73±0.05		
LVAW;s	mm	1.05±0.02	1.08±0.07	0.88±0.06		0.96±0.08		
LVID;d	mm	3.9±0.1	3.8±0.1	4.5±0.1		4.30.1		
LVID;s	mm	2.7±0.1	2.7±0.1	3.8±0.1	**	3.7±0.2	*	
LV Vol;d	µL	65±6	62±5	92±6		83±7		
LV Vol;s	µL	28±4	28±3	63±5		58±7		
EF	%	56±3	55±2	32±2	***	32±2	***	
FS	%	29±2	28±1	15±1	***	15±1	***	
HR	BPM	450±20	471±29	496±19		467±11		
Body Weight	g	20±1	20±1	22±1		21±1		
56 Days Post-Infarction – Endpoint								
LVPW;d	mm	0.67±0.03	0.61±0.02	0.74±0.06		0.74±0.03		
LVPW;s	mm	0.94±0.04	0.91±0.03	0.82±0.08		1.04±0.04		††
LVAW;d	mm	0.63±0.04	0.77±0.05	0.63±0.10		0.67±0.03		
LVAW;s	mm	1.00±0.05	1.15±0.07	0.72±0.13		1.01±0.08		†
LVID;d	mm	4.19±0.05	4.23±0.09	5.66±0.29	***	5.18±0.13	***	
LVID;s	mm	3.01±0.03	3.06±0.08	5.08±0.35	***	4.05±0.20	**	†††
LV Vol;d	µL	78±2	80±4	162±18	***	129±8	**	†
LV Vol;s	µL	35±1	37±2	130±20	***	74±9		†††
EF	%	54±2	54±2	23±4	***	44±4		†††
FS	%	28±1	28±1	11±2	***	22±2		†††
HR	BPM	475±12	495±26	487±15		489±11		
Body Weight	g	24±2	23±2	27±1		27±2		

C57BL/6 male and female mice were subjected at 8–10 weeks of age to permanent ligation of the left coronary artery or sham survival surgery. Echocardiographic data obtained 2 days after surgery was used to identify mice meeting inclusion criteria. Mice were then randomized into two groups each of sham-operated and infarcted mice. The separate groups of sham-operated and infarcted mice were

injected IV with 5×10^{11} vg AAV9sc.shmAKAP or AAV9sc.shControl the third day after survival surgery. M-mode echocardiography parameters: LVPW, Left ventricular posterior wall thickness; LVAW, left ventricular anterior wall thickness; LVID, Left ventricular internal diameter; d, diastole; s, systole; Vol, Volume; EF, ejection fraction; FS, fractional shortening; BW, body weight; HR, heart rate. As echocardiography data were not obtained for 1 shmAKAP - sham mouse for the −2 and 14 day time points, echocardiography data were analyzed by time-matched ANOVA using a mixed-effects model and Tukey post-hoc testing. Only 2 and 56 day time-point data are shown in this table; see Figure 4 for other time points. All data are mean ± s.e.m.

$^{*}p$ vs. Sham-operated for same AAV;

$^{\dagger}p$ vs. shControl for same surgical procedure.

$^{*,\dagger}p \leq 0.05$;

$^{**,\dagger\dagger}p \leq 0.01$;

$^{***,\dagger\dagger\dagger}p \leq 0.001$.